1.C:1.E.1 *Nuclear Physics* **A165** (1971) 199—210;

α-PARTICLE MODEL OF ^{16}O

G. F. BERTSCH †
Joseph Henry Laboratories,
Princeton University, Princeton, New Jersey 08540 ††
and
W. BERTOZZI
Department of Physics
and
Laboratory of Nuclear Science,
Massachusetts Institute of Technology, Cambridge, Massachusetts 02139 ††

Received 21 December 1970

Abstract: A simple α-particle model is constructed for ^{16}O. By making suitable approximations on the wave function of four interacting particles, we reduce the Schrödinger equation to a one-dimensional equation. The equation is solved using empirical α-α interactions. Reasonable agreement with experiment is obtained on the radius of the ground state, and the energies of the ground and first excited 0^+ states. The model qualitatively explains the predominantly deformed structure of the excited state, and the mixing of a deformed component into the ground state. The value obtained for the mixing is somewhat too large.

1. Introduction

There has been a recent revival of interest in α-models of light nuclei. This is partly due to the failure of the shell model to provide a concise description of nuclear properties. In particular, the low-lying even parity states of ^{16}O have been difficult to understand since their energies are much lower than expected on the basis of single-particle energies. The accumulated data about the electromagnetic properties of these states has further emphasized the complex nature of this nucleus. One example is the existence of a rotational band encompassing the states 0^+ (6.06 MeV), 2^+ (6.91 MeV), 2^+ (9.85 MeV), 3^+ (11.08 MeV), 4^+ (10.35 MeV), 6^+ (16.2 MeV), 4^+ (16.8 MeV), and requiring strong triaxial deformation [11,16]). Evidence that a fair amount of this component is admixed in the ground state is provided by the strong E2 transition from the 2^+ state at 6.91 MeV. Along with other features, this adds further complication to an already challenging situation for the shell-model theory. A shell-model representation of the 0^+ state of ^{16}O at 6.06 MeV is discussed by Brown

† Alfred P. Sloan Foundation Fellow 1969-71.
†† Work supported in part by the U.S. Atomic Energy Commission under Contract AT-(30-1)-2098 and by the Air Force Office of Scientific Research under Contract AF 49 (638)-1545.

and Green [1]), using mainly a 4p-4h state. This state has a particular mixture of shell configurations giving a triaxially deformed density distribution. The number of configurations needed to describe this state is very large, and an even greater number would be needed to calculate the energy of the state. To obtain a wave function usable for discussing the electromagnetic properties, mixing is required between this state, a similar 2p-2h state, and the closed-shell state. As we will see, the α-models provide a much more transparent description of such dynamics.

Two kinds of α-models may be distinguished, the α-particle model and the α-cluster model [2]). The α-particle model, which we apply to ^{16}O in this paper, is conceptually very simple. We ignore the fact that α-particles are made up of nucleons, and just treat the dynamics of point α-particles interacting through some phenomenological potential. This model has some difficulties which have not yet been fully resolved. First, α-α potentials are necessarily non-local. There is a short-range repulsion between α-particles which comes from exclusion effects and is therefore non-local. Taking the potential from phase-shift data, we can never be certain of the specific nonlocality. Also, non-local potentials are difficult to handle in the Schrödinger equation. However, two phenomenological potentials have been published which limit the nonlocality to a dependence of the potential on angular momentum [3,4]). Fitting the phase-shift data of α-α scattering, these authors find that the S-wave had a repulsive core inside of 2 fm. The inner repulsion of the potential of Ali and Bodmer [3]) decreases with higher L, as to be expected from an exclusion effect.

A second possible difficulty of the α-particle model is that the α-particles might polarize strongly while they interact. Then we would be forced to consider effective 3α interactions, based on the changes in the pair interaction in the vicinity of a third particle. This possibility could render the model useless, but we are optimistic that such effects are not important. For one thing, the binding energy of an α-particle exceeds the average interaction energy of an α-pair by a factor of ten. The binding energy of the nuclei ^{12}C-^{28}Si can be explained in the α-model with roughly constant nuclear interaction energy of nearby α-particles [5]). Strong polarization effects would cause the three-α interaction to be important in heavier nuclei.

Some insight into the relation between the α-particle model and the shell model is obtained from the α-cluster model [2]). Like the shell model, the cluster model has wave functions consisting of Slater determinants of nucleon wave functions. The orbits are assumed to be Gaussians centered about different points in configuration space, and the α-clusters are groups of four of these single-particle orbits. In the limit of strongly overlapping clusters, the (regular) tetrahedral α-configuration of ^{16}O becomes the shell-model state of the oscillator model, and a planar diamond configuration becomes the deformed 4p-4h shell-model state used by Brown and Green. These shapes are illustrated in fig. 1. Antisymmetrization must be performed explicitly in the cluster model, and several clusters must be considered together for a complete wave function. The calculations with this model are quite promising in reproducing the static properties of nuclei, such as binding energies and r.m.s. radii, but the cluster

model does not seem well suited to the description of the dynamics of the α-particles.

The simpler α-particle model has been extensively applied to ^{12}C, where existing three-body techniques may be applied [6]). It is interesting that the physics of the first two 0^+ states seems quite similar for this nucleus as for ^{16}O. The ground state is

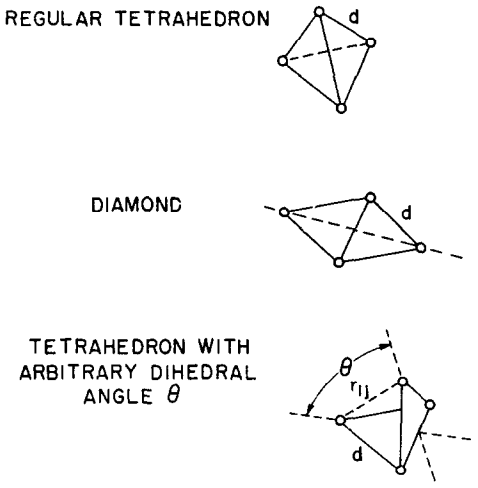

Fig. 1. Configurations of four α-particles.

mostly a compact, triangular configuration, while the 7.6 MeV 0^+ state is largely a "chain" configuration, obviously highly deformed in shape [7]). We will attempt to find a wave function for ^{16}O with a four-body Schrödinger equation, but unlike the three-body problem, the Hamiltonian is quite intractable without several rather drastic approximations. We will develop the approximations necessary to find a wave function, and then compare properties with experiment and other models. We shall find that the structure is close to a regular tetrahedron in the ground state and close to a planar diamond in the excited state.

2. The Hamiltonian

We start with the four-body Schrödinger Hamiltonian,

$$H = -\sum_{4} \frac{\hbar^2}{2m_\alpha} \nabla_i^2 + \sum_{6} V(r_{ij}), \tag{1}$$

where V_{ij} is the interaction between α-particles.

An immediate reduction of the Hamiltonian is possible by transforming to a coordinate system with the twelve cartesian coordinates replaced by the three c.m. coordinates, three Euler angle coordinates giving the orientation of the α-configuration, and six remaining internal coordinates. We take these internal coordinates to be the six relative separation distances of the four α-particles.

The element of phase space in this coordinate system is given by

$$\prod_i^4 \mathrm{d}^3 x_i = \mathrm{d}^3 X_{\mathrm{c.m.}} \mathrm{d}^3\Omega \frac{\prod_{ij}^6 r_{ij}\,\mathrm{d}r_{ij}}{6V}, \tag{2}$$

where V is the volume of the tetrahedron defined by the α-particles. In terms of the internal coordinates, the intrinsic Hamiltonian is

$$H_{\mathrm{int}} = \sum^6 \left(-\frac{\hbar^2}{2m_\alpha} \frac{1}{r_{ij}^2} \frac{\partial}{\partial r_{ij}} r_{ij}^2 \frac{\partial}{\partial r_{ij}} + V(r_{ij}) \right) - \frac{\hbar^2}{2m} \sum_{\text{adjacent sides}}^{12} 2 \frac{\boldsymbol{r}_{ij} \cdot \boldsymbol{r}_{kl}}{r_{ij} r_{kl}} \frac{\partial}{\partial r_{ij}} \frac{\partial}{\partial r_{kl}}. \tag{3}$$

We have not defined the Euler angles or included them in (3). Thus this Hamiltonian can only describe states with no dependence on orientation, i.e. 0^+ states. However, as mentioned in the introduction, there is much experimental evidence on the first two 0^+ states of ^{16}O which we could hope to reproduce.

With the above intrinsic coordinate system, it is natural to approximate the ground state wave function by the form

$$\psi_0 \approx \prod_{ij}^6 \varphi(r_{ij}). \tag{4}$$

This expression has the correct permutation symmetry and describes a 0^+ state. Approximations of this type were introduced by Wigner and are discussed by Hall and Post [8]). For the excited state, we assume a wave function of the form

$$\psi_1 \approx \frac{1}{\sqrt{6}} \sum_{ij} \varphi'(r_{ij}) \prod_{kl}^5 \varphi(r_{kl}). \tag{5}$$

In principle these wave functions could be found by a Hartree-Fock technique. That is, we would take the expectation of the Hamiltonian with a trial wave function of the form (4); integrate out all the coordinates except one, and vary the wave function in that coordinate to minimize the expectation value. This results in a one-dimensional Schrödinger equation to be solved with self-consistent input parameters. Unfortunately, the above coordinate system is not suited to a straightforward solution of the problem by this method. From (2) we see that there is a singularity in the phase-space volume element when all particles lie in a plane. This implies that the $\varphi(r_{ij})$ will have singularities at some maximum and minimum values of r_{ij}. However, it is possible to remove the singularity in a particular coordinate r_{ij} by a further coordinate transformation. Consider the α-configuration as a tetrahedron composed of two triangles lying on a common base, with apices joined by the coordinate r_{ij}. If instead of r_{ij} we use the angle between the two triangles to describe the tetrahedron, the phase-space volume element has the non-singular form,

$$\frac{\prod^6 r_{ij}\,\mathrm{d}r_{ij}}{6V} = \frac{\prod^5 (r_{mn}\,\mathrm{d}r_{mn})\mathrm{d}\theta_{ij}}{r_{kl}}, \qquad kl \text{ opposite } ij. \tag{6}$$

The derivatives in the kinetic energy operator are then replaced by

$$\frac{\partial}{\partial r_{ij}} \to \frac{\partial\theta}{\partial r_{ij}} \frac{\partial}{\partial\theta},$$
$$\frac{\partial}{\partial r_{mn}} \to \frac{\partial\theta}{\partial r_{mn}} \frac{\partial}{\partial\theta} + \frac{\hat{\partial}}{\partial r_{mn}} \qquad mn \neq ij. \tag{7}$$

With this replacement the Hamiltonian is reduced by parametrizing its dependence on all coordinates except θ. Integrations over the other coordinates are simulated by replacing r_{ij} by d, an average separation distance, and $\boldsymbol{r}_{mn} \cdot \boldsymbol{r}_{kl}/r_{mn}r_{kl}$ by its value for two equilateral triangles joined at the bases. With this reduction the Hamiltonian for the θ-variable becomes

$$H_{\text{red}} = H_0 + H',$$

with

$$H_0 = -\frac{\hbar^2}{2m_\alpha} \frac{\partial}{\partial\theta} \frac{1+\sin^2\frac{1}{2}\theta}{\frac{3}{4}d^2} \frac{\partial}{\partial\theta} + V(\sqrt{3}d \sin\tfrac{1}{2}\theta), \tag{8}$$
$$H' = -\frac{\hbar^2}{2m_\alpha} \sum_{mn} \frac{\sin\frac{1}{2}\theta\cos\frac{1}{2}\theta}{\sqrt{\frac{3}{4}}d} \frac{\partial}{\partial r_{ij}} \frac{\partial}{\partial\theta}.$$

We notice that the term H' in the kinetic energy operator couples the different coordinates. This is very different from the usual situation in Hamiltonian dynamics; normally the kinetic energy operator is separable in the coordinates, while the potential energy couples the coordinates together. We shall consider two approximations: a) we neglect the coupling entirely and, b) we treat the off-diagonal matrix elements of the coupling in second-order perturbation theory. The diagonal matrix elements of the coupling will be small if the φ-functions are sufficiently localized. Including the off-diagonal terms in second-order perturbation theory yields an effective Hamiltonian for the θ-coordinate:

$$H_{\text{eff}} = H_0 + E^{(2)},$$

with

$$E^{(2)} = \sum_{mn} \frac{\langle\varphi(r_{mn})|H'|\varphi'(r_{mn})\rangle^2}{E_\varphi - E_{\varphi'}}. \tag{9}$$

When this perturbation is evaluated treating the $\varphi(r_{im})$ as oscillator functions, we find an amusing result: the inertia of the augmented Hamiltonian is identical to the inertia of the corresponding classical rigid motion [9]). Explicitly, the Hamiltonian (9) reduces to

$$H_{\text{eff}} = -\frac{\hbar^2}{m_\alpha} \frac{\partial}{\partial\theta} \frac{8}{3d^2(1+\cos^2\frac{1}{2}\theta)} \frac{\partial}{\partial\theta} + V(\sqrt{3}d \sin\tfrac{1}{2}\theta). \tag{10}$$

The coefficient of the θ-derivative is just the classical inertia associated with the hinge motion of two rigid triangles joined at their bases.

3. Wave functions

The symmetry of the 0^+ wave function implies the boundary condition on the $\varphi(\theta)$ function

$$\frac{\mathrm{d}\varphi(\theta)}{\mathrm{d}\theta}|_{\theta=0,\pi} = 0. \tag{11}$$

We will solve the Schrödinger equation with the Hamiltonian (10), using the above boundary condition, and the potential of Ali and Bodmer [3]). The parameter d is determined self-consistently by making an approximate identification between r_{ij} and θ,

$$r_{ij} = \sqrt{3}d \sin\theta. \tag{12}$$

The output $\theta(\varphi)$ will imply a $\varphi(r)$ from which a new value of d can be obtained.

A second parameter is necessary in the calculation because of the angular momentum dependence of the potential. The angular momentum of pairs in the wave function (3) will not be pure. Ideally the specific mixture of different L-values could be determined by projection. However, we resort to a simpler and possibly inaccurate method. We estimate the transverse kinetic energy of a pair and assume an angular momentum structure the same as for plane waves of the same kinetic energy. Our potential energy function thus has a parameter T, the average kinetic energy of a pair. The potential is explicitly

$$V = \frac{\sum (2L+1)[j_L(kr_{ij})]^2 V_L(r_{ij})}{\sum_L (2L+1)[j_L(kr_{ij})]^2}, \qquad k = \sqrt{\frac{Tm_\alpha}{\hbar^2}}. \tag{13}$$

The parameters d and T may be found by fitting the wave functions to Gaussians:

$$\varphi \approx \exp\left[-\left(\frac{r-r_0}{a}\right)^2\right], \qquad T = 2\hbar^2/m_\alpha a^2, \qquad d = r_0. \tag{14}$$

The overlap of the θ-eigenfunction with a Gaussian is high, in the vicinity of 0.99. The best fit to d and a parameters resulting are plotted in figs. 2 and 3. We are very fortunate in that the output parameters are not sensitive to the input parameters. The self-consistent values are $d = 3.4$ and $T = 9.2$ MeV. The wave function of a nearby set of parameters is shown as the solid line in fig. 4. Note that the wave function peaks near 70.5°, the dihedral angle of a regular tetrahedron. However, the wave function is rather diffuse in angle.

We now turn to a discussion of the ground state binding energy. The 2α system is unbound by 95 keV, while the binding of heavier nuclei can be attributed to an α-α

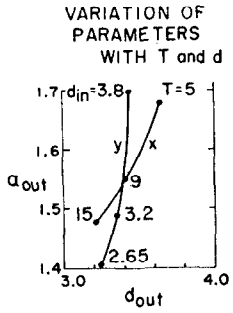

Fig. 2. The variation of the parameters of the best-fit Gaussian wave function, $\varphi \approx \exp[-(r-d)^2/a^2]$, with the input parameters in the Schrödinger equation. Curve x shows the values of d and a resulting from varying T and holding the input d fixed at 3.4 fm. Curve y shows the variation with d, holding T fixed at 9.2 MeV. The variation is due mainly to the differences in binding energies with the different parameter sets.

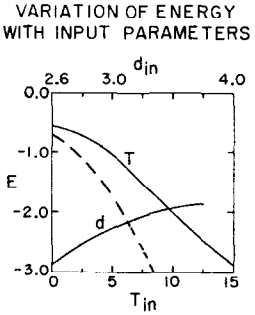

Fig. 3. The energy of the ground state of H_{eff}, as a function of parameters T (holding d fixed at 3.2 fm) and of d (holding T fixed at 9.2 fm).

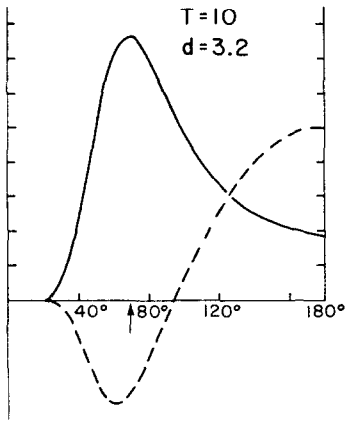

Fig. 4. Eigenfunctions of H_{eff}. The solid line is the ground state and the broken line the first excited state of the Hamiltonian. The arrow indicates the dihedral angle of a regular tetrahedron.

interaction of about 2.5 MeV. The eigenenergies of the Schrödinger equation, which should reproduce this experimental interaction, are given in table 1. Although we

TABLE 1

Interaction energies of α-particles in ^{16}O

Hamiltonian interaction	H_0	$H_0+E^{(2)}=H_{\text{eff}}$	Hall-Post lower bound
S-wave parameters for all partial waves	−0.36	−0.60	−1.75
S+D+G of Ali and Bodmer [ref. [3])]	−1.68	−2.05	−3.78

The experimental value is −2.4 MeV per α-pair.

have calculated wave functions with the Hamiltonian (10), this is not the correct Hamiltonian to use for the pair energy, since it counts the perturbation term twice. (This is the same overcounting problem familiar from Hartree-Fock theory.) We quote in the table the lowest eigenenergies of H_0 and H_{eff}. The effect of the angular momentum dependence of the potential is quite strong. The S-wave potential by itself gives far too little binding, but the self-consistent potential gives binding in the neighbourhood of the experimental value. The dependence of the energy on the input parameters d and T is shown in fig. 3. We also calculated the energies with the Benn and Sharf potential, replacing the hard cores by finite repulsion. The S-wave part is almost exactly the same, but the higher partial waves made the interaction too strong at physical values of the parameter T. The results for this potential are illustrated by the dashed line in fig. 3. We feel that this potential is not as reliable as that of Ali and Bodmer because of the unphysical nature of the hard core and oscillations in higher partial waves. Nevertheless, it is discouraging that two potentials that fit the phase shifts do not give exactly the same binding.

The strong T-dependence makes the calculation quite unreliable for the interaction energy. We can only say that the model reproduces the correct binding to within a half an MeV or so. Finally, the Hall-Post [8]) lower bound on the α-α interaction is listed in the last column of the table. The bound proves that a purely local potential fitting the S-wave phase shifts is too weak. For reasonable angular momentum mixtures, the bound seems to overestimate the energy by an MeV or so.

The first excited state of the Hamiltonian (12) has a wave function shown in fig. 4 with a broken line. The peak of the wave function is at the planar configuration of the α-particles, the shape found with the shell-model theory and the α-cluster calculations of the lowest excited 0^+. It perhaps goes against intuition that the maximum of the wave function should lie away from the potential well. We can understand this effect by recalling that semiclassically the wave function amplitude goes inversely as the square root of the velocity of the particles. At the planar configuration of this

state, the particles are out of the well and moving relatively slowly. The eigenenergy of this wave function with the Hamiltonian (10) is 5 MeV above the ground state, in reasonable agreement with the experimental 6.06 MeV excitation energy of the second 0^+ state. However, for this state it is not legitimate to neglect the coupling term in the Hamiltonian, since there could be substantial diagonal matrix elements with the wave function (4).

It is interesting to compare these wave functions with the molecular model, which assumes small amplitude vibrations of the α-particles about the tetrahedral shape. Using this model, Dennison [10]) assigned many states in the spectrum of ^{16}O to vibrational and rotational states of a tetrahedron. In particular, the 6.06 MeV state was interpretated as a monopole (purely radial) vibration. Using wave functions of the type (4) and (5), the model requires that φ and φ' are well localized at a particular r, the length of the tetrahedron. Wave function (4) is the ground state, and we can see that (5) is the monopole vibration, because it is the only symmetric way to excite one vibrational quantum. Thus, if Dennison's model were valid, it would emerge from our calculations of φ and φ'. Our function φ perhaps is localized well enough, but the φ' we find from the Schrödinger equation certainly is not. While radial motion is the only permitted motion in the vicinity of the tetrahedral shape, it is energetically very unfavourable for large amplitudes, since it separates all α-particles. The hinge motion, separating only one pair, requires less energy.

4. Matrix elements and conclusion

Elastic and inelastic electron scattering gives quite detailed information on the distribution of charge in the ground state and transition charge density connecting the ground and 6.06 MeV state [11]). In the α-model, the form factor can be written as a product

$$F(q) = F_\alpha(q) F_m(q), \tag{15}$$

where F_α is the form factor of the α-particle itself and F is the form factor of the α-structure in terms of the α-coordinates:

$$F_m = \int \prod_i^4 \mathrm{d}^3 r_i \, \mathrm{e}^{\mathrm{i}qr_i} \psi^*(r_i \ldots) \psi(r_i \ldots). \tag{16}$$

At low momentum transfer, only the mean square radius of the charge distribution is needed to characterize the form factor,

$$F_s^{0\to 0} = 1 - \tfrac{1}{6}\langle R^2\rangle_{00} q^2, \qquad F_s^{0\to 1} = \tfrac{1}{6}\langle R^2\rangle_{01} q^2. \tag{17}$$

We calculate the mean square radius in the α-model using the relation between the square radius of a tetrahedron and the lengths of its sides,

$$\sum_4 (r_i - r_{\mathrm{c.m.}})^2 = \tfrac{1}{4} \sum_{ij} r_{ij}^2. \tag{18}$$

The matrix elements of r_{ij} are evaluated in the θ-coordinate system, assuming the remaining coordinates can be integrated out

$$\langle\varphi|r_{ij}^2|\varphi'\rangle = \int \mathrm{d}\theta\varphi(\theta)3d^2\sin^2\tfrac{1}{2}\theta\varphi'(\theta). \tag{19}$$

Taking into account the finite size the α-particle, we obtain for the mean square radius of the ground state

$$\langle R^2\rangle = \langle R^2\rangle_\alpha + \tfrac{3}{2}\langle\varphi|r_{ij}^2|\varphi\rangle. \tag{20}$$

Our result, quoted in table 2, looks very accurate, but actually the structure part

TABLE 2
Matrix elements of $R^2 = \Sigma_p r_p^2$

	α-model with $d = 3.3$, $T = 9.2$	Experiment
$\sqrt{1/Z\langle\text{g.s.}\|R^2\|\text{g.s.}\rangle}$	2.79 fm	2.67 fm [ref. [12])]
$\langle\text{g.s.}\|R^2\|6.06\rangle$	7.9 fm^2	3.8 ± 0.3 fm^2

$\langle R^2\rangle_{00}$, is too large by about 15 %. The transition mean square radius may be computed with the wave functions (4) and (5) and is given by

$$\langle R^2\rangle_{01} = \tfrac{3}{2}\sqrt{6}\langle\varphi|r_{ij}^2|\varphi'\rangle. \tag{21}$$

The result, 7.9 fm^2, is too large by a factor of two. Another α-particle calculation [13]) which assumes pure radial motion overestimates the transition matrix element by a factor of 4. On the other hand the shell-model estimates are too low by a similar factor, unless some ill-defined effects on single-particle wave functions are included in the calculation †. The fact that our value for the transition matrix element is too large indicates that the nucleus is actually more rigid than the α-model predicts. In the usual shell-model approximations, the nucleus is far too rigid an object. So we conclude that the truth is somewhere in between: a shell-model calculation with a greatly augmented basis or an α-calculation allowing for single-particle structure would have a good chance of success in reproducing the transition matrix element.

The underlying convergence of the shell-model and α-methods is strikingly illustrated by a graphical comparison of the wave functions in fig. 5. The shell-model amplitude of the 0p-0h and 4p-4h components correspond respectively to α-configurations of tetrahedral and diamond shapes [2]). The phases of these components were compared via the α-cluster model. It is plausible to assume that the 2p-2h state has a

† The single-particle effects included are core polarization and the deviation of sd shell orbits from the oscillator form. It is possible to improve the agreement with the experimental data either with a core polarization prescription [14]) or with the use of Woods-Saxon wave function for the sd orbitals [15]).

highest overlap with an α-configuration of some intermediate angle. On the plot of the $\varphi(\theta)$ we can schematically superimpose the three shell-model amplitudes as wave packets in the θ-coordinate. The amplitudes of the shell-model wave functions have the magnitudes given by Brown and Green. The α-model wave function is normalized

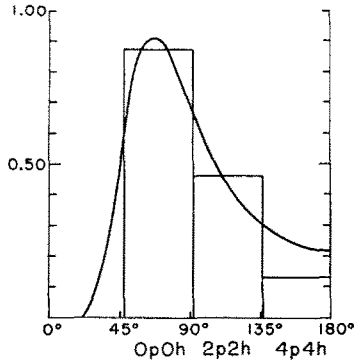

Fig. 5. Comparison of shell-model and α-model wave functions of ground state. See text for explanation.

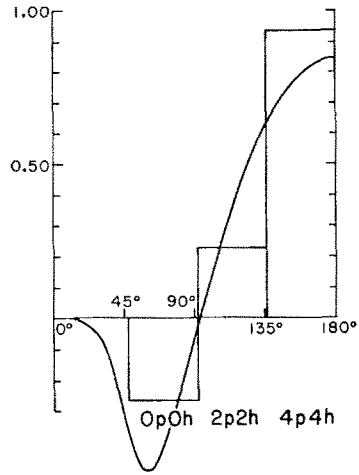

Fig. 6. Comparison of shell-model and α-model wave functions of excited 0^+ state.

to have the same probability integral as the Brown and Green wave function. We see a remarkable similarity in the wave functions, the main difference being a quantitative one that the α-model wave function is too spread out. This is an example of a collective coordinate, θ, which provides a useful description of a complicated wave function and shows the dynamics underlying the shell-model mixing.

It is also interesting to compare the approximation schemes of the shell and α-model. In first order the shell model treats the kinetic energy operator very well, but

does a rather poor job on the potential energy, since correlations are neglected. In contrast, the α-model does very well on potential energy with all the α-correlations built in, but cannot describe the kinetic energy very well as long as the α-particles are fixed. To improve the dynamical description, the shell model uses the potential as a perturbation. Thus from the shell-model point of view, it is a potential energy that mixes three components of ^{16}O. In the α-particle model the different shapes are mixed by the kinetic energy operator. It is quite satisfying that the same final picture emerges from two diametrically opposite approaches to the Hamiltonian problem.

References

1) G. E. Brown and A. M. Green, Nucl. Phys. **75** (1966) 401
2) See D. M. Brink, The alpha-particle model of light nuclei, International School of Physics, "Enrico Fermi" Course XXXVI;
D. M. Brink, H. Friedrich, A. Weiguny and C. W. Wong, Phys. Lett. **33** (1970) 143
3) S. Ali and A. R. Bodmer, Nucl. Phys. **80** (1966) 99
4) J. Benn and G. Scharf, Helv. Phys. Acta **40** (1967) 271
5) L. R. Halstad and E. Teller, Phys. Rev. **54** (1938) 681
6) See J. V. Noble, Phys. Lett. **31B** (1970) 253 and references cited
7) H. Hebach and P. Henneberg, Z. Phys. **216** (1968) 204
8) R. L. Hall and H. R. Post, Proc. Phys. Soc. **90** (1967) 381
9) G. F. Bertsch, Ann. of Phys., to be published
10) D. Dennison, Phys. Rev. **57** (1940) 454; **96** (1954) 378
11) J. C. Bergstrom *et al.*, Phys. Rev. Lett. **24** (1970) 152
12) H. F. Ehrenberg *et al.*, Phys. Rev. **113** (1959) 666
13) J. V. Noble, Phys. Rev. **C1** (1970) 1900
14) W. J. Gerace and D. A. Sparrow, Nucl. Phys. **A154** (1970) 576
15) B. Buck, private communication
16) G. J. Stephenson and M. K. Banerjee, Phys. Lett. **24B** (1967) 209;
G. J. Stephenson, Jr., Theoretical problems in low energy reactions, Nuclear research with low energy accelerators (Academic Press, New York, 1967)